Ordering in the Subphase of a Langmuir Monolayer: X-ray Diffraction and Anomalous Scattering Studies

ARTICLE · AUGUST 2001

DOI: 10.1021/la010518w

6 AUTHORS, INCLUDING:

Alokmay Datta
Saha Institute of Nuclear Physics
123 PUBLICATIONS **1,112** CITATIONS
SEE PROFILE

Andrew G. Richter
Valparaiso University (USA)
56 PUBLICATIONS **991** CITATIONS
SEE PROFILE

Ordering in the Subphase of a Langmuir Monolayer: X-ray Diffraction and Anomalous Scattering Studies

Jan Kmetko,* Alokmay Datta,† Guennadi Evmenenko, Mary K. Durbin,‡ Andrew G. Richter,§ and Pulak Dutta

Department of Physics & Astronomy, Northwestern University, Evanston, Illinois 60208-3112

Received April 6, 2001. In Final Form: May 13, 2001

The properties of amphiphilic organic monolayers ("Langmuir films") at the air−water interface are strongly affected by metal ions in the aqueous subphase, and such monolayers can be used as templates to grow oriented crystals from dissolved salts. Our synchrotron X-ray studies of fatty acid monolayers spread on a dilute aqueous solution of lead ions indicate that a ∼5 Å thick ordered layer is formed in the subphase. The lattice is commensurate with the organic lattice and has 14 times the unit cell area. It is unlikely that lead ions alone would form such a large repeat unit; indeed, using anomalous X-ray scattering, we detect no evidence of lead within the ordered layer. Thus, the interfacial superlattice is not simply an array of lead ions but may consist of lead hydrolysis products and water molecules.

Introduction

The properties of an organic amphiphilic monolayer floating at the air−water interface can change significantly when metal ions are added to the subphase. The monolayer generally becomes much better ordered,[1] changes its viscoelastic response,[2] and transfers more easily to a solid substrate.[3] These "Langmuir films" have been used as templates for the nucleation and growth of oriented three-dimensional inorganic crystals, a model biomineralization process.[4−8] The ordering of various ions under Langmuir films and in Langmuir−Blodgett (transferred) films has been investigated using X-rays,[9,10] surface potential measurements and surface light scattering,[11] infrared reflection−absorption spectrometry,[12] and atomic force microscopy.[13] With a cadmium salt dissolved in the subphase, formation of a monolayer lattice in the subphase has been observed using X-ray diffraction.[9,10] Since the superlattice is seen only in the presence of subphase Cd^{2+} ions, it is tempting to conclude[9,10] that the superlattice must be an ordered array of Cd^{2+} ions. However, there is no chemically specific evidence of the composition of the superlattice, and the unit cell is quite large (a 2 × 3 supercell of the Langmuir monolayer unit cell). We sought to learn more about this initial stage of bulk inorganic nucleation by studying fatty acid Langmuir films with Pb^{2+} ions in the subphase, using X-ray scattering. Lead is a heavy atom that scatters X-rays strongly and (unlike cadmium) has an experimentally accessible (L3) absorption edge; this latter fact allowed us to perform anomalous X-ray scattering studies that directly test for the presence of lead in the superlattice.

Experiment

The experimental setup and procedures for data collection and analysis were similar to those described elsewhere.[14] Grazing incidence diffraction (GID) studies were performed at the 1-BM-C (bending magnet) beamline of SRI-CAT at the Advanced Photon Source, Argonne National Laboratory. The X-ray beam was vertically focused to a width of 600 μm and horizontally unfocused (horizontal width ∼1 cm). The beam was deflected downward at an incident angle of ∼1.8 mrad to the water surface, just below the critical angle for total external reflection from water, to reduce background scattering. Vertical and horizontal soller slits in front of the detector defined a horizontal resolution of ∼0.01 $Å^{-1}$ full width at half-maximum (fwhm) for K_{xy} scans and a vertical resolution of ∼0.05 $Å^{-1}$ fwhm for K_z scans. Diffraction and rod scan data are presented after subtracting the background.

Water purified to 18 MΩ cm resistivity by a Barnstead Nanopure Infinity deionization system was used to prepare the subphase. A dilute aqueous solution containing 10^{-5} M lead chloride (Sigma, quoted purity 99.999%) was dissolved in the subphase whose pH was not adjusted and measured to be ∼5.5. About 65 μL of a 0.87 mg/mL solution of heneicosanoic acid ($C_{20}H_{41}COOH$ or C_{21}, Sigma, quoted purity 99%) in chloroform was spread at the air−solution interface of the subphase. C_{21} is a saturated straight-chain molecule; its chemical diagram is given in ref 15, Figure 1a. The phase diagram of pure C_{21} is well-known,[15] so effects due to the lead ion can be easily discerned. A mechanical barrier compressed the monolayer to a pressure of about 0.5 dynes/cm (i.e., essentially zero pressure) at 10 °C, and the film was left to equilibrate for an hour. All scans were performed at constant pressure, at about 0.5 dynes/cm. Surface pressure (π) was measured with ±0.2 dyn/cm accuracy (Balance ST9000, Nima Technology). A slight overpressure of helium was maintained in the trough to reduce radiation damage and air

* To whom correspondence should be addressed. E-mail: j-kmetko@northwestern.edu.

† Present address: Saha Institute of Nuclear Physics, Calcutta 700064, India.

‡ Present address: ADAC Laboratories, 540 Alder Drive, Milpitas, CA 95035.

§ Present address: Advanced Photon Source, Argonne National Laboratory, Argonne, IL 60439.

(1) Schwartz, D. K. *Surf. Sci. Rep.* **1997**, *27*, 241.

(2) Ghaskadvi, R. S.; Carr, S.; Dennin, M. *J. Chem. Phys.* **1999**, *111*, 3675.

(3) Zasadzinski, J. A.; Viswanathan, R.; Madsen, L.; Garnaes, J.; Schwartz, D. K. *Science* **1994**, *263*, 1726.

(4) Rapaport, H.; Kuzmenko, I.; Berfeld, M.; Kjaer, K.; Als-Nielsen, J.; Popovitz-Biro, R.; Weissbuch, I.; Lahav, M.; Leiserowitz, L. *J. Phys. Chem. B* **2000**, *104*, 1399.

(5) Mann, S. *Nature* **1993**, *365*, 499.

(6) Heywood, B. R.; Mann, S. *Adv. Mater.* **1994**, *6*, 9.

(7) Zhao, X. K.; Yang, J.; McCormick, L. D.; Fendler, J. H. *J. Phys. Chem.* **1992**, *96*, 9933.

(8) Litvin, A. L.; Valiyaveettil, S.; Kaplan, D. L.; Mann, S. *Adv. Mater.* **1997**, *9*, 124.

(9) Leveiller, F.; Jacquemain, D.; Lahav, M.; Leiserowitz, L.; Deutsch, M.; Kjaer, K.; Als-Nielsen, J. *Science* **1991**, *252*, 1532.

(10) Leveiller, F.; Böhm, C.; Jacquemain, D.; Möhwald, H.; Leiserowitz, L.; Kjaer, K.; Als-Nielsen, J. *Langmuir* **1994**, *10*, 819.

(11) Yazdanian, M.; Yu, H.; Zografi, G.; Kim, M. W. *Langmuir* **1992**, *8*, 630.

(12) Gericke, A.; Hühnerfuss, H. *Thin Solid Films* **1994**, *245*, 74.

(13) Garnaes, J.; Schwartz, D. K.; Viswanathan, R.; Zasadzinski, J. A. *Nature* **1992**, *357*, 54.

(14) Datta, A.; Kmetko, J.; Yu, C. J.; Richter, A. G.; Chung, K. S.; Bai, J. M.; Dutta, P. *J. Phys. Chem. B* **2000**, *104*, 5797.

(15) Kaganer, V. M.; Möhwald, H.; Dutta, P. *Rev. Mod. Phys.* **1999**, *71*, 779.

10.1021/la010518w CCC: $20.00
Published on Web 07/03/2001

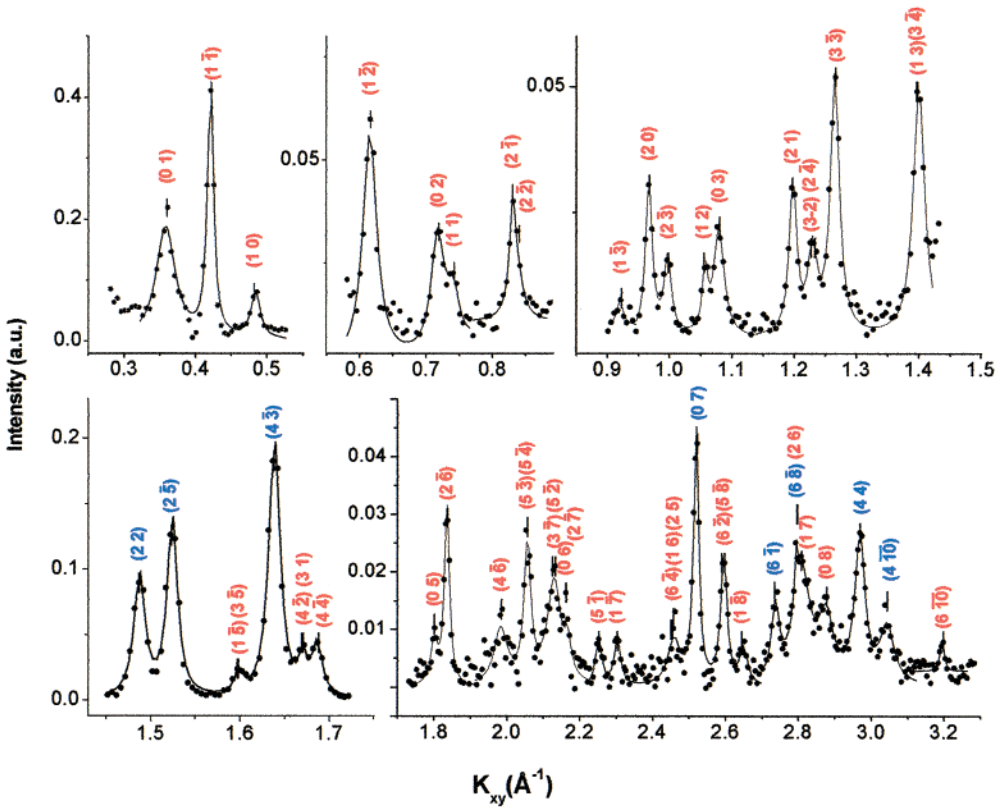

Figure 1. Grazing incidence synchrotron X-ray diffraction data from a heneicosanoic acid Langmuir monolayer with lead ions in the subphase. The lower-order peaks (2 2), (2 $\bar{5}$), and (4 $\bar{3}$), labeled in blue, correspond to the reciprocal lattice of the Langmuir monolayer (this identification is made from Bragg rod scans; see Figure 2). The higher-order peaks (0 7), (6 $\bar{1}$), (6 $\bar{8}$), (4 4), and (4 $\overline{10}$), labeled in blue, are also from the Langmuir monolayer. All other peaks are due to the superlattice.

Table 1. Observed In-Plane Positions of Bragg Peaks in the GID Pattern[a]

		K_{xy}(Å^{-1})				K_{xy}(Å^{-1})				K_{xy}(Å^{-1})				K_{xy}(Å^{-1})	
h	k	calculated	observed	h	k	calculated	observed	h	k	calculated	observed	h	k	calculated	observed
0	1	0.3597	0.360	2	$\bar{2}$	1.2292	1.229	2	$\bar{6}$	1.8344	1.835	5	$\bar{8}$	2.5893	2.593
1	$\bar{1}$	0.4217	0.422	2	4	1.2332		4	$\bar{6}$	1.9866	1.986	6	$\bar{2}$	2.5925	
1	0	0.4840	0.484	3	$\bar{3}$	1.2651	1.263	5	4	2.0519	2.052	1	$\bar{8}$	2.6511	2.649
1	$\bar{2}$	0.6166	0.616	3	$\bar{4}$	1.3960	1.399	5	$\bar{3}$	2.0576		**6**	**$\bar{1}$**	**2.7291**	**2.730**
0	2	0.7194	0.719	1	3	1.3986		5	$\bar{2}$	2.1251	2.128	**6**	**$\bar{8}$**	**2.7919**	
1	$\bar{1}$	0.7412	0.742	**2**	**$\bar{2}$**	**1.4825**	**1.484**	3	$\bar{7}$	2.1322		2	6	2.7972	**2.794**
2	$\bar{1}$	0.8335	0.833	**2**	**$\bar{5}$**	**1.5210**	**1.521**	0	6	2.1582	2.161	1	7	2.8062	
2	$\bar{2}$	0.8434		1	$\bar{5}$	1.5937	1.598	2	$\bar{7}$	2.1623		**4**	**4**	**2.9650**	**2.962**
1	$\bar{3}$	0.9172	0.920	3	$\bar{5}$	1.5987		5	$\bar{1}$	2.2487	2.252	**4**	**$\overline{10}$**	**3.0421**	**3.042**
2	0	0.9680	0.967	**4**	**$\bar{3}$**	**1.6379**	**1.637**	1	$\bar{7}$	2.2964	2.299	6	$\overline{10}$	3.1974	3.196
2	$\bar{3}$	0.9933	0.993	4	$\bar{2}$	1.6671	1.667	1	6	2.4509	2.457				
1	2	1.0599	1.058	3	1	1.6719		2	$\bar{5}$	2.4555					
0	3	1.0791	1.079	4	$\bar{4}$	1.6868	1.686	6	$\bar{4}$	2.4584					
2	1	1.1992	1.199	0	5	1.7985	1.800	**0**	**7**	**2.5179**	**2.521**				

[a] There are 39 distinct peaks in the in-plane diffraction pattern, and they are listed under the "observed" column. Bold labels indicate positions of peaks primarily due to the organic film. Some peak positions are so close to each other that they cannot be distinguished as separate peaks in our data, Figure 1 (note that the monolayers are powders in the plane). Studies of multiple films gave peak positions reproducible to ±0.002 Å^{-1}. The "calculated" column contains peaks calculated from the magnitudes of the (0 1), (1 $\bar{1}$), and (1 0) basis vectors; these magnitudes were refined by maximizing the overall agreement between all calculated and observed peaks.

scattering. To reduce radiation damage further, fresh subphase solution and monolayer were prepared after an hour of X-ray exposure.

Results and Discussion

In-plane diffraction scans revealed a total of 39 distinct peaks (Figure 1). This observation is qualitatively similar to that reported in ref 9 (in the presence of subphase Cd^{2+}), but there are many more peaks and the peak positions are different. The lowest observed peak is at 0.36 Å $^{-1}$, indicating the appearance of a much larger unit cell than that of a Langmuir monolayer.

There are three relatively strong peaks in the K_{xy} region of ~1.5 Å^{-1}, indexed[16] (2 2), (2 $\bar{5}$), and (4 $\bar{3}$) and so labeled in Figure 1 and marked in bold in Table 1. We performed scans along the Bragg rods at these peaks (i.e., we measured the scattered intensity above background as a function of K_z with K_{xy} held constant at the peak positions). The width of a Bragg rod is inversely proportional to the thickness of the monolayer;[15] specifically, the intensity profile along K_z can be approximated[17] by $I_{hk}(K_z) \approx$

(16) We used a basis that results in integer (hk) for all peaks; if we had indexed in terms of the triangular lattice of the Langmuir monolayer, these peaks would have been (0 1), (1 $\bar{1}$), and (1 0), respectively.

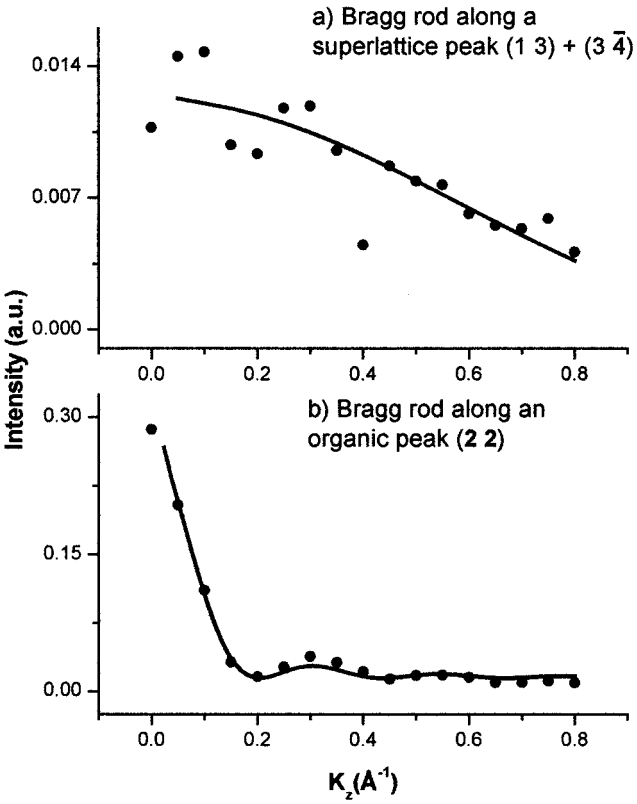

Figure 2. (a) Bragg rod scan of a representative in-plane peak along a superlattice "inorganic" peak (1 3) + (3 $\bar{4}$). We have obtained similar Bragg rod scans at other superlattice peaks: (0 2), (1 1), (1 $\bar{5}$) + (3 5), and (4 $\bar{2}$) + (3 1). (b) Bragg rod scan of a representative in-plane peak along a peak due to the organic monolayer (2 2). We have obtained similar Bragg rod scans at the other two low-order "organic" peaks: (2 $\bar{5}$) and (4 $\bar{3}$). The intensities fall off more sharply in (b), indicating that the peak originates from a thicker film (~27 Å) compared to the Bragg rod in (a), which indicates a thickness of ~5 Å.

Table 2. Thickness Calculated from Fits to Bragg Rods[a]

h k	thickness (Å)	*h k*	thickness (Å)
(0 2)	4.8	**(2 $\bar{5}$)**	**27**
(1 1)	4.9	(1 $\bar{5}$) + (3 $\bar{5}$)	3.6
(1 3) + (3 $\bar{4}$)	4.9	**(4 $\bar{3}$)**	**27**
(2 2)	**27**	(4 $\bar{2}$) + (3 1)	2.5

[a] Bragg rods along these seven peaks were fitted with $I_{hk}(K_z) \approx I_0(\sin W/W)^2$ where $W = {}^1/_2LK_z$ and L is the thickness. The organic peaks (shown in bold) indicate a thickness of 27 Å, consistent with the length of the molecule. Bragg rods for the five "inorganic" peaks studied yield a much smaller layer thickness, ~5 Å or less.

$I_0(\sin W/W)^2$ where $W = {}^1/_2LK_z$ and L is the thickness. Fits to the Bragg rods of any of the three strong peaks (Figure 2b) yielded a thickness of 27 Å (Table 2), consistent with the length of the heneicosanoic acid molecule. This confirms that these strong peaks are primarily due to the packing of fatty acid molecules. In addition, the intensity maxima along the Bragg rods are at or near $K_z = 0$, which means that the acid molecules are untilted (normal to the plane of the interface). These diffraction peaks indicate an oblique unit cell with dimensions $a = 4.52$ Å, $b = 4.99$ Å, $\gamma = 121.9°$, and an area of 19.15 Å^2, with one organic molecule per unit cell.[18] There are also five relatively strong peaks in the region $K_{xy} > 2.5$ Å^{-1}, indexed (0 7), (6 $\bar{1}$), (6 $\bar{8}$), (4 4), and (4 $\overline{10}$), that are higher order diffraction peaks from the same structure[19] (these are also marked in bold in Table 1).

The Bragg rods along the remaining peaks (Figure 2a, Table 2) are consistently much wider than those along the three strong peaks (Figure 2b), which means that these peaks are from a much thinner layer (thickness ~5 Å). These weak in-plane reflections correspond to a superstructure with cell dimensions $a' = 15.35$ Å, $b' = 20.66$ Å, $\gamma' = 122.25°$, and an area of 268.1 Å^2. These parameters were refined by maximizing the overall agreement between all calculated and observed peaks.

Since the area of the supercell is exactly 14 times that of the organic unit cell and since the organic lattice peaks are also peaks of the superlattice (i.e., a common indexing scheme can be employed), the two lattices must be commensurate. A schematic representation of the organic cell and the supercell in real space is shown in Figure 3. The relative orientation of the two lattices is determined by the fact that this is the only way they can be commensurate: the shortest real-space basis vectors of the organic cell (**a**, **b**) and inorganic cell (**a**′, **b**′) are related by the vector identities $\mathbf{a}' = 4\mathbf{a} + 2\mathbf{b}$ and $\mathbf{b}' = -3\mathbf{a} + 2\mathbf{b}$.

Although we have observed and indexed a large number of diffraction peaks, these peaks do not tell us the type and arrangement of atoms within a single supercell. A determination of even a crude trial-and-error supercell structure from peak intensities would require some knowledge of its atomic composition. Rather than simply assuming that the lattice is an array of lead ions (cf. refs 9 and 10), we sought to test for the presence of lead within the superlattice. If the superlattice peaks were solely due to lead ions, the contribution to the intensity of each weak peak should be proportional to the square of the lead form factor. Tuning the X-ray energy from 12.885 keV (below the L3 absorption edge of the lead atom) to 13.100 keV (slightly above the edge) reduces the lead form factor[20] from $f = 70.21 + 4.187i$ to $f = 62.18 + 10.13i$, and so the absolute intensity of a diffraction peak due to scattering from lead atoms should decrease by ~20%. We have measured the intensities of 13 weak peaks with K_{xy} between 0.6 and 1.4 Å^{-1} at these two energies (data for some representative superlattice peaks and also some organic lattice peaks[21] are shown in Figure 4). Within an experimental error of ~5%, we observed no change for any of these peaks.

This unexpected result means that the simple picture of electrostatic or covalent bonding of individual metal ions to the amphiphile headgroups is inadequate. Since lead does not contribute measurably to the diffraction peak intensity, scattering from the superstructure must be dominated by other atoms. In principle, superlattice reflections can arise from a periodic superstructure within the organic monolayer. For example, small superstructures attributed to protruding ends of the fatty acid molecules because of periodic buckling have been observed in films on solid substrates by AFM.[3] Protrusions of the organic molecules have also been observed in polymer−lipid monolayers at the air−water interface,[22] although no superlattice has been reported. However, the Bragg

(17) Kjaer, K.; Als-Nielsen, J.; Helm, C. A.; Tippman-Krayer, P.; Möhwald, H. *J. Phys. Chem.* **1989**, *93*, 3200.

(18) The nonprimitive cell with two organic molecules, normally centered-rectangular (ref 15), is a parallelogram in the presence of lead ions.

(19) In terms of the alternate indexing system mentioned earlier (ref 16), these would have been (1 $\bar{2}$), (1 1), (2 1), (0 2) and (2 $\bar{2}$), respectively.

(20) Kissel, L. *Radiat. Phys. Chem.* **2000**, *59*, 185.

(21) Of course, we do not expect the scattering from organic molecules to be affected in any way as the energy passes through the lead absorption edge. Indeed the strong peaks, which are primarily due to scattering from the Langmuir monolayer, did not change. This confirms that our diffraction intensities are reproducible.

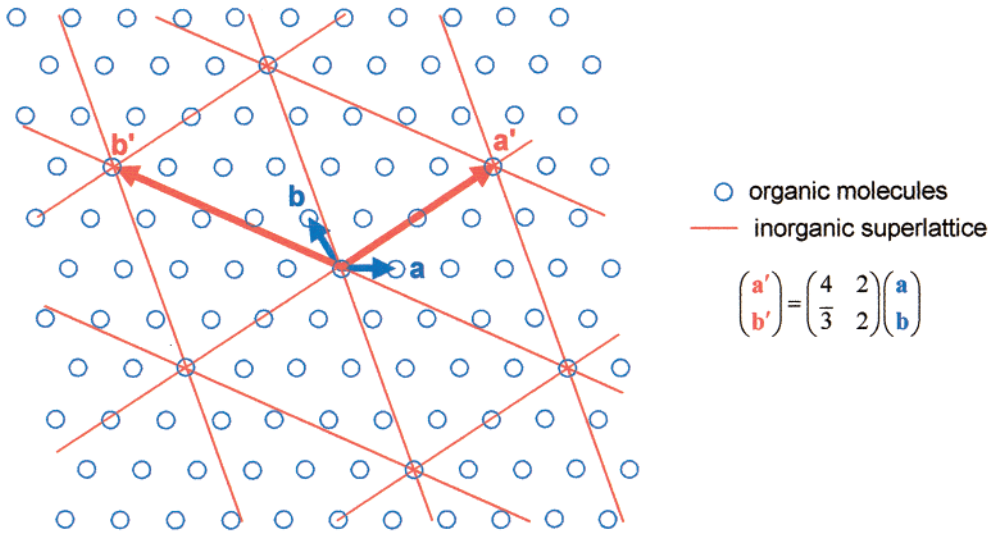

Figure 3. Real space lattices of the fatty acid monolayer and the superlattice. The heneicosanoic acid molecules are represented by circles; the lattice parameters are $a = 4.52$ Å, $b = 4.99$ Å, and $\gamma = 121.9°$, so that area = 19.15 Å^2. The superstructure is shown by lines; the lattice parameters are $a' = 15.35$ Å, $b' = 20.66$ Å, $\gamma' = 122.25°$, and area′ = 268.1 Å^2. The lattices are commensurate: the basis vectors are related through $\mathbf{a}' = 4\mathbf{a} + 2\mathbf{b}$ and $\mathbf{b}' = -3\mathbf{a} + 2\mathbf{b}$, so that area′ = 14 × area.

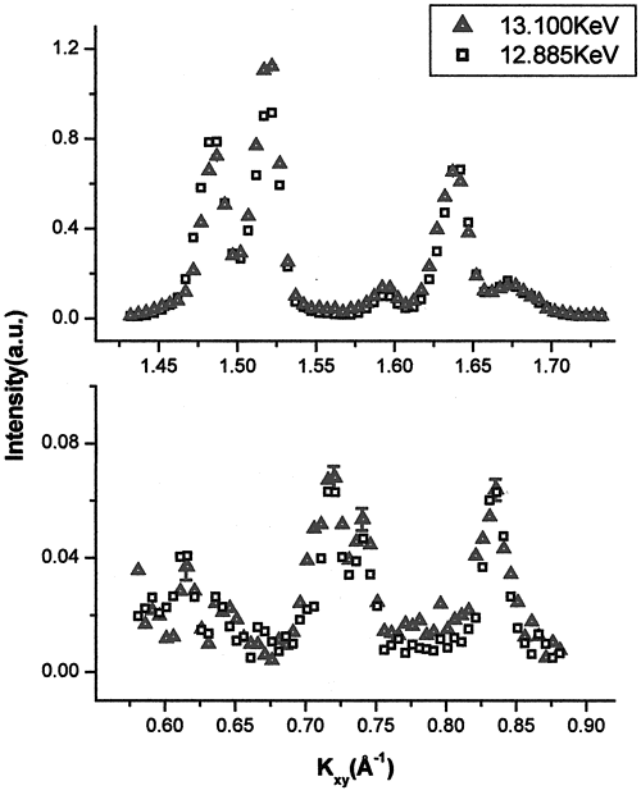

Figure 4. In-plane diffraction scan with X-ray energy below and slightly above the L3 absorption edge of lead: (a) three peaks from the organic monolayer (ref 21) plus weak superlattice peaks and (b) four representative superlattice peaks. We also looked at nine other superlattice peaks not shown here, with the same results. If the superlattice consisted of lead atoms only, a 20% change in the peak intensities would be expected. There was no observable change in intensity for any of the peaks studied.

rod widths we observe (Figure 2a) are not consistent with horizontal or vertical density modulations in the entire organic monolayer.

The only reasonable possibility is that the superlattice peaks are due to a thin layer in the aqueous subphase. Since no superlattice is seen when no multivalent metal ions are added to the subphase (even at very high pH), different lattices are seen when different ions are added, and the results are insensitive to the exact water purity (we have used commercial distilled water on occasion), the lattice cannot be due to impurities in the water. However, it is well established[23] that metal ions undergo hydrolysis and hydration in aqueous solution, and a wide range of complex polynuclear oxo(hydroxo)-bridged structures can be formed. The observation of changes in the organic monolayer structure as a function of the subphase pH and subphase ion concentration[14] is further evidence that pH- and concentration-sensitive hydrolysis products, rather than isolated ions, are present at the interface. Thus, we expect that hydrolysis products and water molecules arrange themselves under the Langmuir monolayer, interacting with the carboxyl headgroups in such a way as to form a large commensurate superlattice. In this picture, the ratio of lead atoms to other atoms (hydroxyl ions, water) can be small enough that their presence is undetectable in our anomalous scattering studies. We suspect that the same thing happens in the presence of many other ions, such as cadmium[9] or silver,[24] as well.

Our results indicate that the process of ion−headgroup complexation may be more complicated than has been previously assumed. Further experiments with spectroscopic techniques that are sensitive to the chemical nature of the inorganic complexes, such as grazing incidence extended X-ray absorption edge fine structure (EXAFS), may be useful to identify the ionic species. Diffraction experiments on Langmuir films with other ions in the subphase are currently under way.

Acknowledgment. This work was supported by the U.S. Department of Energy under Grant No. DE-FG02-ER45125. It was performed at Sector I (SRI-CAT) of the Advanced Photon Source.

LA010518W

(22) Majewski, J.; Kuhl, T. L.; Kjaer, K.; Gerstenberg, M. C.; Als-Nielsen, J.; Israelachvili, J. N.; Smith, G. S. *J. Am. Chem. Soc.* **1998**, *120*, 1469−1473.

(23) Richens, D. T. *The chemistry of aqua ions*; Wiley: New York, 1997; Chapter 2.5.4.

(24) Weissbuch, I.; Baxter, P. N. W.; Kuzmenko, I.; Cohen, H.; Cohen, S.; Kjaer, K.; Howes, P. B.; Als-Nielsen, J.; Lehn, J. M.; Leiserowitz, L.; Lahav, M. *Chem.—Eur. J.* **2000**, *6*, 725.